AGU ADVANCING EARTH AND SPACE SCIENCES

Geophysical Research Letters

RESEARCH LETTER
10.1029/2025GL115856

The Santorini 2024–2025 Volcano-Tectonic Sequence: Constraining the Initial Phase of the Intra-Caldera Unrest

C. Papazachos[1], **M. Foumelis**[1], **S. Bitharis**[2], **Ch. Pikridas**[2], **E. Trasatti**[3], **E. Papageorgiou**[1], **Ch. Ventouzi**[1], **Ch. Kkallas**[1], **G. Vougioukalakis**[4], **and O. Vaselli**[5]

[1]School of Geology, Aristotle University Thessaloniki, Thessaloniki, Greece, [2]School of Rural and Surveying Engineering, Aristotle University Thessaloniki, Thessaloniki, Greece, [3]Istituto Nazionale di Geofisica e Vulcanologia, Rome, Italy, [4]Hellenic Authority of Geology & Mineral Exploration (EAGME), Athens, Greece, [5]Department of Earth Sciences, University of Florence, Florence, Italy

Key Points:

- In 2024 Santorini experienced an intra-caldera unrest after 2011, with a seismic swarm on the Kameni fault line and radial deformation
- Synthetic Aperture Radar Interferometry and GNSS data constrain a deformation source at 3.4 km b.s.l., in the northern Santorini caldera low velocity (melt storage) area
- The seismicity and deformation patterns, as well as the inferred magma (deformation) source, are very similar to the previous 2011 unrest

Supporting Information:

Supporting Information may be found in the online version of this article.

Correspondence to:

C. Papazachos,
kpapaza@geo.auth.gr

Citation:

Papazachos, C., Foumelis, M., Bitharis, S., Pikridas, C., Trasatti, E., Papageorgiou, E., et al. (2025). The Santorini 2024–2025 volcano-tectonic sequence: Constraining the initial phase of the intra-caldera unrest. *Geophysical Research Letters*, *52*, e2025GL115856. https://doi.org/10.1029/2025GL115856

Received 12 MAR 2025
Accepted 19 JUN 2025

Author Contributions:

Conceptualization: C. Papazachos, M. Foumelis, S. Bitharis, Ch. Pikridas, E. Trasatti, G. Vougioukalakis, O. Vaselli
Data curation: C. Papazachos, M. Foumelis, S. Bitharis, Ch. Pikridas, E. Trasatti, E. Papageorgiou, Ch. Ventouzi, Ch. Kkallas, G. Vougioukalakis, O. Vaselli
Formal analysis: C. Papazachos, M. Foumelis, S. Bitharis, Ch. Pikridas, E. Trasatti, E. Papageorgiou, Ch. Ventouzi, Ch. Kkallas, G. Vougioukalakis, O. Vaselli
Investigation: C. Papazachos, M. Foumelis, S. Bitharis, Ch. Pikridas,

Abstract After less than 14 years from the previous 2011–2012 unrest, the Santorini volcano entered a new unrest phase, involving intra-caldera deformation since July 2024 and microseismicity mainly after mid-September 2024. We examine the first phase of this unrest, identified by GNSS and Synthetic Aperture Radar Interferometry data as an almost radial expansion of the northern caldera by ~7 cm within 6 months (7/2024–12/2024). The unrest also involves a seismic swarm along an 8 km × 6 km segment of the Kameni line fault, with events up to M_L3.8. We model the inflation with a near-vertical spheroid at a depth of ~3.4 km, resulting in a 6+ million m^3 expansion within 6 months. While the proposed deformation source is almost identical for the two unrests, which also show similar seismicity and deformation trends, we do not observe the significant increase of H_2 emissions associated with the 2011–2012 unrest.

Plain Language Summary Nearly 14 years after 2011, when Santorini went through volcanic unrest for 14 months, a similar phenomenon occurs since July 2024. This involves a small-magnitude earthquake swarm within the caldera, along a fault formed by historical eruption centers (Kameni line). Moreover, we observe a radial expansion and vertical uplift of the whole island (especially the northern Santorini caldera), identified by GNSS stations and satellite Synthetic Aperture Radar Interferometry (InSAR) data. We model this deformation with a magmatic body intrusion of 6+ million m^3 at a depth of ~3.4 km within 6 months. This body is located within the northern Santorini caldera melt storage area, previously identified by seismic tomography, very close to a similar body to which the 2011–2012 unrest has been attributed. Since Santorini has been slowly deflating before 2011, as well as between the two unrests, as shown by GNSS and InSAR data, we observe a consistent pattern involving quick inflation periods and longer intervals of slow deflation between the unrests. As caldera eruptions are always preceded by unrest (though most unrests do not lead to an eruption), it is necessary to maintain an improved real-time monitoring of the volcano to identify any future pre-eruptive patterns.

1. Introduction

Santorini volcano (Figure 1a) is part of the Hellenic Volcanic Arc, generated by the subduction of the eastern Mediterranean microplate beneath the Southern Aegean. While submarine volcanic activity started ~0.65 Myr ago, Santorini became highly explosive after ~0.3 Myr, with at least twelve Plinian or super-Plinian eruptions with an inter-event period >20,000 years (e.g., Druit et al., 2019). Although its last Late Bronze Age eruption dates back ~3,600 years (Pearson et al., 2018), at least nine historical eruptions occurred within the Santorini caldera until 1950 (Georgalas, 1953), building the intra-caldera islets of Palea and Nea Kameni (Pyle & Elliott, 2006; Vougioukalakis & Fytikas, 2005).

Early work on the Santorini caldera using Synthetic Aperture Radar Interferometry (InSAR) data suggests the absence of noteworthy magma intrusions from 1992 to 2010 (Papageorgiou et al., 2012), except from a possible small-scale subtle aseismic inflation in the northwest caldera section (Stiros et al., 2010). Intra-caldera seismicity has also been very low since at least 1994 (Dimitriadis et al., 2005, 2009), when the Institute for the Study and Monitoring of the Santorini Volcano (ISMOSAV) was established, allowing the systematic monitoring of the volcano by local networks (seismological, GNSS, etc.) and InSAR.

A significant volcano-tectonic unrest occurred between January 2011 and March 2012, with low magnitude earthquakes ($M_L \leq 3.2$) predominantly occurring along the Kameni line (Papadimitriou et al., 2015; Tassi

E. Trasatti, E. Papageorgiou, Ch. Ventouzi, Ch. Kkallas, G. Vougioukalakis, O. Vaselli
Methodology: C. Papazachos, M. Foumelis, S. Bitharis, Ch. Pikridas, E. Trasatti, E. Papageorgiou, Ch. Ventouzi, Ch. Kkallas, G. Vougioukalakis, O. Vaselli
Resources: C. Papazachos, M. Foumelis, S. Bitharis, Ch. Pikridas, E. Trasatti, E. Papageorgiou, Ch. Ventouzi, G. Vougioukalakis, O. Vaselli
Software: C. Papazachos, M. Foumelis, S. Bitharis, Ch. Pikridas, E. Trasatti, E. Papageorgiou, Ch. Ventouzi, Ch. Kkallas, G. Vougioukalakis, O. Vaselli
Supervision: C. Papazachos, M. Foumelis, S. Bitharis, Ch. Pikridas, E. Trasatti
Validation: C. Papazachos, M. Foumelis, S. Bitharis, Ch. Pikridas, E. Trasatti, E. Papageorgiou, Ch. Ventouzi, Ch. Kkallas, G. Vougioukalakis, O. Vaselli
Visualization: C. Papazachos, M. Foumelis, S. Bitharis, Ch. Pikridas, E. Trasatti, E. Papageorgiou, Ch. Ventouzi, Ch. Kkallas, G. Vougioukalakis, O. Vaselli
Writing – original draft: C. Papazachos, M. Foumelis, S. Bitharis, Ch. Pikridas, E. Trasatti, Ch. Ventouzi
Writing – review & editing: C. Papazachos, M. Foumelis, S. Bitharis, Ch. Pikridas, E. Trasatti, E. Papageorgiou, Ch. Ventouzi, Ch. Kkallas, G. Vougioukalakis, O. Vaselli

et al., 2013), and changes in topography and soil gas flux and composition (e.g., Parks et al., 2013; Tassi et al., 2013). GPS (Newman et al., 2012) and InSAR data (Foumelis et al., 2013; Parks et al., 2012, 2015) identified a significant uplift, reaching 14 cm within a year due to a magmatic body intrusion in the northern Santorini caldera at the depth of ~3.5–4 km (e.g., Foumelis et al., 2013; Newman et al., 2012; Parks et al., 2012, 2015; Saltogianni et al., 2014). This unrest did not lead to an eruption; geodetic and seismic data indicated that the unrest slowed down to pre-unrest levels, with post-unrest degassing after mid-2012 (Papageorgiou et al., 2019; Saltogianni et al., 2014).

Since mid-summer 2024, Santorini has experienced a complex and unprecedented volcano-tectonic unrest, consisting of two phenomena: (a) a new, low-seismicity intra-caldera unrest since early July 2024, and (b) an intense volcano-tectonic seismic sequence, mainly occurring in the broader Anydros islet area, ~30 km to the northeast of Santorini since late January 2025. Both phenomena were still evolving when this manuscript was compiled. We employed information from the permanent monitoring seismic and GNSS networks (Figure 1a), as well as InSAR and in-situ soil gas data to constrain the intra-caldera unrest until the end of January 2025, since the ensuing Anydros sequence almost completely masked the intra-caldera phenomenon. We also discuss the similarities of the current unrest with the 2011–2012 event, as well as its significance for a possible future eruption.

2. Data and Methodology

2.1. Intra-Caldera Seismicity

Seismicity is monitored by the local seismic network (Figure 1a), jointly operated by ISMOSAV and Aristotle Univ. Thessaloniki (AUTh), with additional stations from the Hellenic Unified Seismological Network (HUSN). We relocated local seismicity hypocenters until the end of January 2025 with Hypoinverse (Klein, 2002), using a 1D model based on available 3D local (Dimitriadis et al., 2010; Heath et el., 2019) and regional models (C. B. Papazachos and Nolet, 1997). Local magnitudes (M_L) were estimated using regional calibrations (Scordilis et al., 2016). Although the relocated intra-caldera events were well-constrained (location errors <1 km for events with $M_L > 1$), we improved hypocentral parameters by double-difference relocation (HypoDD, Waldhauser & Ellsworth, 2000), resulting in formal hypocentral errors <100 m. While this estimate is optimistic, considering the strong local 3D velocity variations (Hooft et al., 2019), it confirms the high-quality of the final hypocenters (Figure 1).

The relocated seismicity (Figures 1b and 1c) suggests that the activated Kameni line fault segment is sub-vertical (dipping to the north), located at the depth of 3–9 km, with a total activated length of ~8 km, slightly longer than the segment activated in 2011–2012 (Papadimitriou et al., 2015; Tassi et al., 2013; Vougioukalakis et al., 2016). A seismicity cluster is identified off-fault (toward Thirasia), while minor seismicity also occurred at shallow depths on the main Santorini island. The on-fault sequence shows two clusters beneath the Kameni islands and the main Santorini urban centers (Fira-Imerovigli-Firostefani), similar to the first 4 months of the 2011–2012 unrest. The largest events were strongly felt on the island, with the M_L3.8 earthquake near Thirasia (dotted ellipse in Figures 1d and 1e) being the most significant.

2.2. GNSS and InSAR Data Processing

We obtained precise daily positions for the available GNSS data for the period 01/2023–01/2025, using the GAMIT-GLOBK software (Herring et al., 2015) in a two-step approach (Bitharis et al., 2024). Initially, we estimate the daily loosely constrained GNSS position solutions for 15 stations. Five are located on Santorini (ISMOSAV GNSS network and Hellenic POsitioning System, HEPOS). The remaining ten correspond to well-distributed stations from the International GNSS Service and EUREF Network (EPN, Bruyninx et al., 2019), used as a reference frame to stabilized the loosely-constrained GNSS solution within the ITRF2014 coordinate system (Altamimi et al., 2016). To retrieve the intra-caldera Santorini deformation, we removed the mean ITRF2014 velocity (tectonic signal) between January 2023 and May 2024 (pre-unrest period) from the daily topocentric coordinates of the whole study period.

We processed the entire Sentinel-1 archive (S1A and S1B satellites) from the European Space Agency and performed interferometric analysis spanning nearly ten years (04/2015–12/2024), securing a dense temporal stack, with ~465 acquisitions per orbital track (ascending-A029 and descending-D109 orbits). Early-phase interferometric processing with the SNAPPING PSI service (Foumelis et al., 2022) on the Geohazards

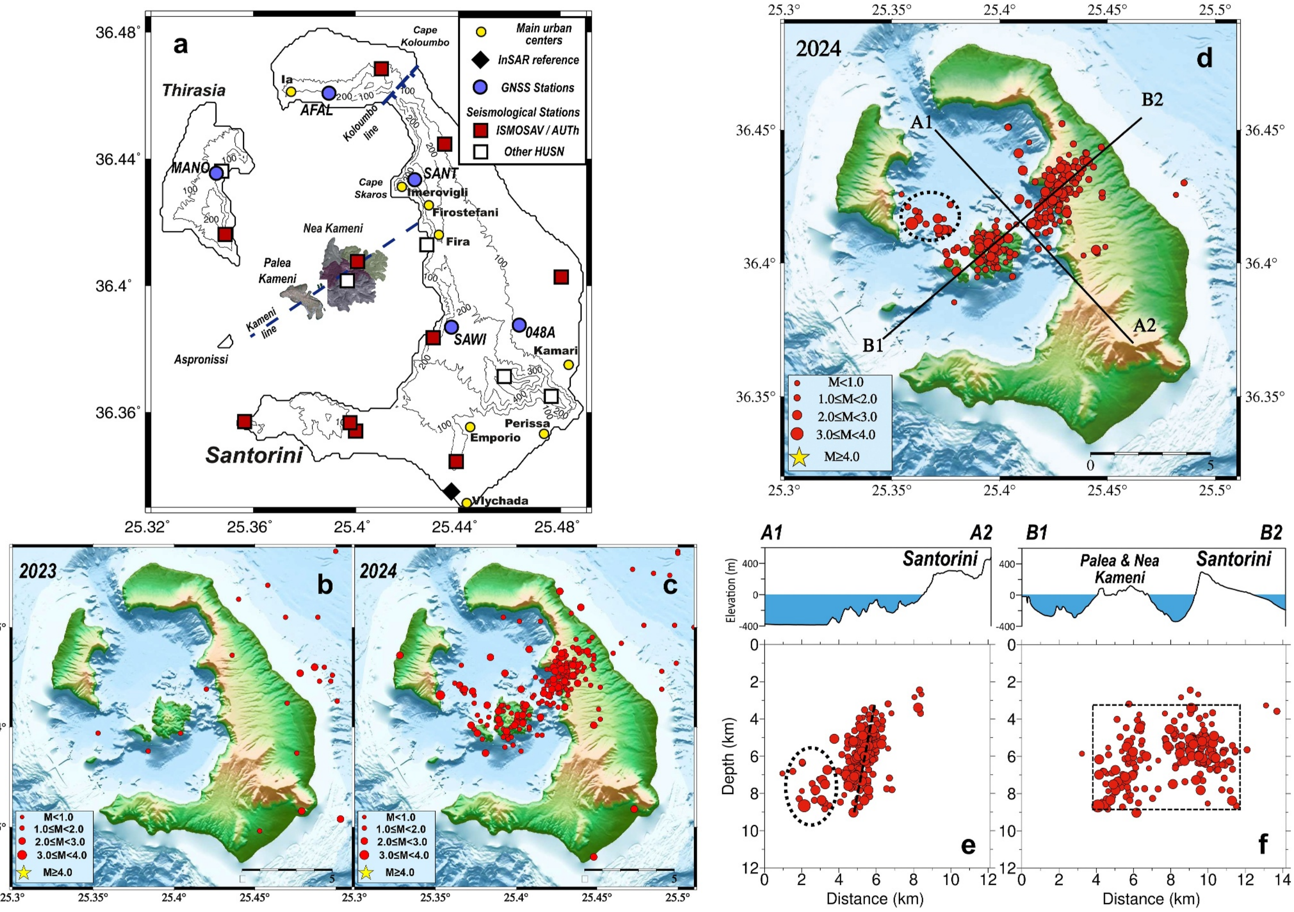

Figure 1. (a) The Santorini volcanic complex: The two main volcano-tectonic lines (Kameni and Koloumbo) and urban centers are depicted with dashed lines and yellow circles, respectively. Squares and blue circles correspond to seismological and GNSS stations, respectively, while the diamond depicts the synthetic aperture radar interferometry reference site (b, c) Santorini seismicity in 2023 and 2024. (d) Intra-caldera seismicity for 2024, after double-difference relocation. (e, f) Seismicity distribution on the strike-normal (A1–A2) and along-strike (B1–B2) profiles depicted in (d), showing the activated sub-vertical Kameni fault. The fault dimensions and dip are delineated with dashed lines in (e) and (f), while the Thirasia off-fault cluster is depicted with a dotted ellipse in (d) and (e).

Exploitation Platform (GEP) successfully detected (see Supporting Information S1) the onset of the unrest (Figure S1 in Supporting Information S1). We then employed a Multi-Temporal InSAR approach (Wegmüller et al., 2015; Werner et al., 2003), which involves multi-reference pairs of interferograms, allowing for improved error compensation and tracking of higher motion gradients. We constrained the temporal baselines of the interferometric pairs between 90 and 270 days, using geometric baselines up to 30 m to reduce phase unwrapping and uncompensated topographic effects errors. This excluded a few acquisitions from further analysis, not affecting the time-series continuity. We selected Vlychada, located at southernmost Alpine basement outcrop (see Figure 1), as local reference for phase unwrapping. To avoid motion underestimation from this local reference, we adjusted all measurements using the velocity of GNSS station SANT projected onto the Line-of-Sight (LoS) geometries.

We mapped the displacement field change from the unrest onset in July 2024 (Figure S2 in Supporting Information S1) by splitting observations before and during the unrest, recalculating the corresponding LoS motion rates. Very low uncertainties (1–3 mm/yr) were estimated for both ascending and descending tracks (Figure S3 in Supporting Information S1). Solutions from independent geometries not only served as a verification mechanism but also allowed the LoS motion decomposition into vertical and E-W components (Figure S4 in Supporting Information S1). We considered the Nearest Neighbor Vector approach for this decomposition (Foumelis, 2016), instead of pixel-based analysis, which underestimates motions due to spatial averaging.

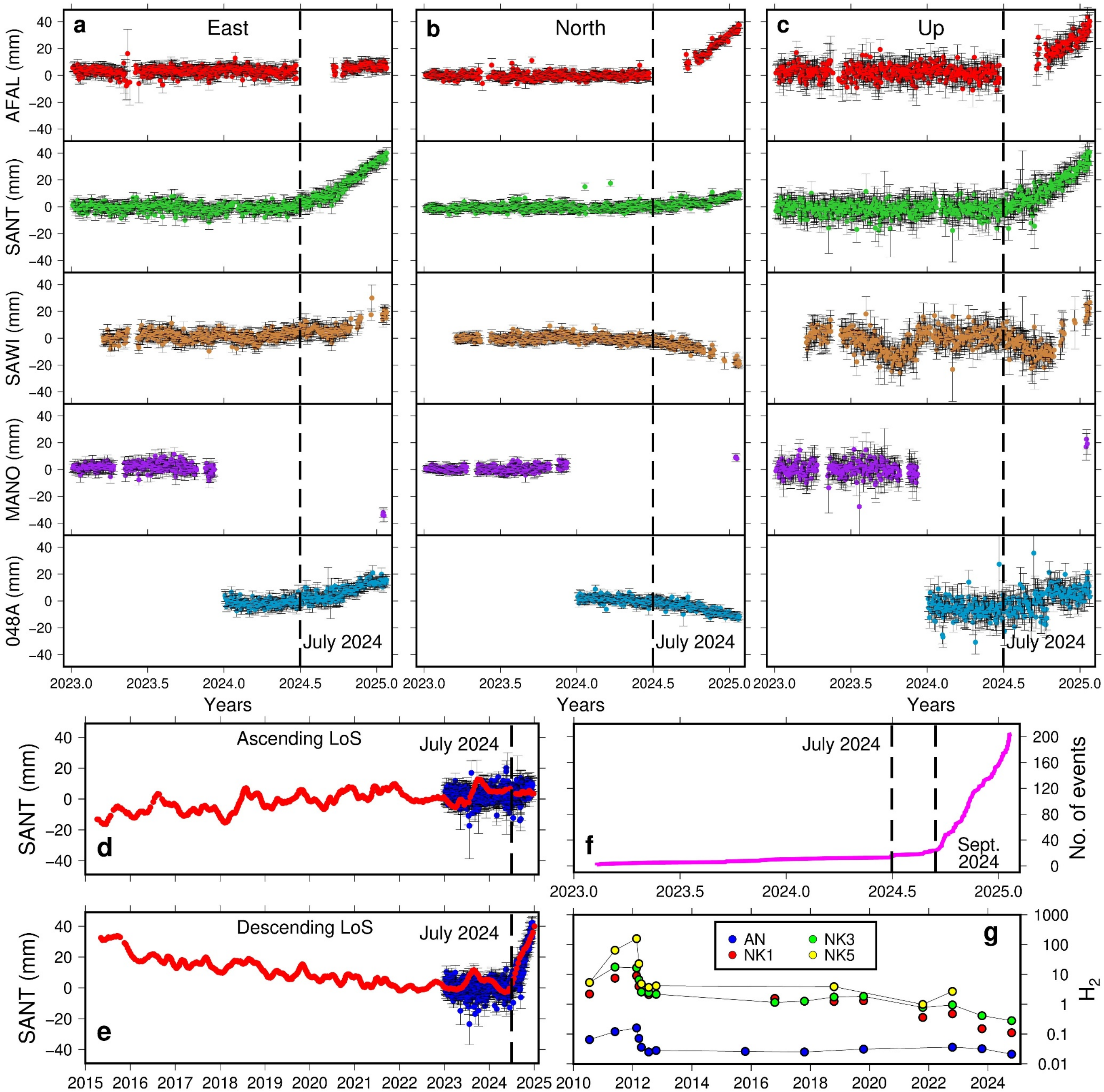

Figure 2. Displacement time series of GNSS stations AFAL, SANT, SAWI, MANO, and 048A for their East (a), North (b) and Up (c) component from 01/2023 to 01/2025. (d, e) Projection of the SANT GNSS 3D components along the ascending and descending satellite LoS directions (blue circles), respectively, with multi-temporal InSAR displacements from 04/2015 to 12/2024 (red lines). (f) Time-variation of the cumulative number of $M_L > 1$ intra-caldera events. (g) H_2 emissions at Nea Kameni fumaroles (NK1, NK3, and NK5) and hot springs (AN). Dashed lines in all subplots mark the unrest onset and low-level seismicity increase (July 2024); the second dashed line in (f) depicts the initiation of high seismicity rate release since mid-September 2025.

3. Results

Figures 2a–2c show the 5 Santorini GNSS time series describing Santorini's internal deformation between 01/2023 and 01/2025. Despite some data gaps, all stations clearly depict a significant uplift since July 2024, with rates between ∼24 and ∼69 mm/yr for a total uplift between ∼13 and ∼38 mm, continuing at a steady rate until late January 2025. The same pattern is observed for the horizontal velocities, with values between ∼40 and

~70 mm/yr and a total radial deformation between ~26 and ~54 mm (Figure 2). Average ITRF2014 horizontal velocities also increased to 56–74 mm/yr for the 5 stations (Table S1 in Supporting Information S1).

The 10-year availability of Sentinel-1 data allowed us to retrieve detailed information on the temporal motion variability, with a distinct changes recognized for the last semester of 2024 in both acquisition geometries (Figure S5 in Supporting Information S1). Specifically, while a downward motion (or motion away from the satellite) is dominant at Nea Kameni until early July 2024, the subsequent period exhibits uplift (or motion toward the satellite). This is also evident from the displacement of GNSS station SANT between 04/2015 and 12/2024 along the ascending and descending satellite LoS directions (Figures 2d and 2e). This motion inversion (Figure 2e) persists over multiple acquisitions (~7 months) at a practically constant rate, consistent with the projected GNSS data. The pattern varies within the Santorini caldera: while the relatively flat topography of Nea Kameni appears to be uplifting in both geometries (Figure S2 in Supporting Information S1), uplift at the western caldera walls (Thirasia) is observed only for the ascending geometry, underlining the important contribution of E-W motion on InSAR results.

A similar variation is observed for the cumulative number of intra-caldera earthquakes with $M_L > 1$ (completeness threshold), showing a small increase in early July 2024, and a significant one after mid-September 2024, with ~1–1.5 events/day until the end of January 2025 (Figure 2f), similar to the 2011–2012 unrest. This later initiation of higher-rate seismicity (2–3 months after the deformation start) is different from the 2011–2012 unrest, where both phenomena started mostly at the same time (January 2011). While H_2 emissions measured in Nea Kameni fumaroles and hot springs increased by almost two orders of magnitude in 2011, they have been at an all-time low level in mid-November 2024, 4.5 months after defomation initiated (Figure 2g).

To further exploit InSAR, we decomposed LoS measurements into vertical and horizontal (E-W) components (Figure 3). The E-W component suggests a convergence toward the northern caldera between 2015 and July 2024, accompanied by deflation of Nea Kameni, not exceeding −8 mm/yr (Figures 3a and 3c), consistent with previously reported post-2011 unrest deflation (Papageorgiou et al., 2019). This pattern changes after July 2024 to extension, with the highest motion rates for the E-W component derived from InSAR data reaching ~120 mm/yr (Skaros cape in the East, northeastern Thirasia in the West). The InSAR findings, together with the observed motion shift to uplift after July 2024, clearly indicate an inflation of the northern Santorini caldera. Moreover, these patterns and rates agree with the GNSS vectors which show a radial extension (Figure 3b), very similar to the 2011–2012 unrest (e.g., Newman et al., 2012). A similar agreement is observed for the InSAR uplift signal, with the highest values found in the northern part of Nea Kameni and Skaros Cape (~120 mm/yr). This uplift is also verified by GNSS estimates, showing uplift rates between 24 and 69 mm/yr.

4. Magma Source Modeling

InSAR and GNSS velocities during the 2024 unrest (07/2024–12/2024) were employed in a non-linear inversion to obtain the deformation source's parameters, using the open-source Python tool VSM (Volcanic and Seismic source Modeling, Trasatti, 2022). This tool combines multi-technique geodetic data sets and sets up a forward model using the most common analytical deformation sources. As a first step, the InSAR data sets were subsampled with an increasing spatial step of 150, 300, and 600 m with respect to a centroid located north of the Kameni islets, resulting in roughly 1,500 data points for each orbit. InSAR and GNSS data misfits were scaled with weights 0.8 and 0.2, respectively, balancing the larger number of SAR data against GNSS benchmarks and the lower GNSS data uncertainty with respect to InSAR (e.g., Trasatti, 2022).

Considering the similarity of the 2024 InSAR and GNSS data (Figure 3) with the 2011–2012 unrest (Foumelis et al., 2013; Newman et al., 2012; Parks et al., 2012, 2015), we employed a prolate spheroidal deformation source (Yang et al., 1988). We generated 80,000 models for the VSM inversion, using a Poisson coefficient of 0.25 and a shear modulus of 10 GPa for the medium following Parks et al. (2015) and Papageorgiou et al. (2019). Preliminary tests with an isotropic point-source and a sill-like source resulted in higher misfits, hence both models were excluded from further analysis. The resulting sub-vertical prolate spheroid (major axis 930 m, aspect ratio 0.4) is located north-west of Kameni islets, at a depth of 3,350 ± 300 m b.s.l (Table S2 in Supporting Information S1). Following the empirical model of Battaglia et al. (2013), we estimated a volume variation rate of 12.5 (±4) x 10^6 m^3/yr, corresponding to more than 6 million m^3 for the 6-month period considered. Figure S7 in Supporting Information S1 reports the 1D and 2D marginal distributions of the obtained model parameters,

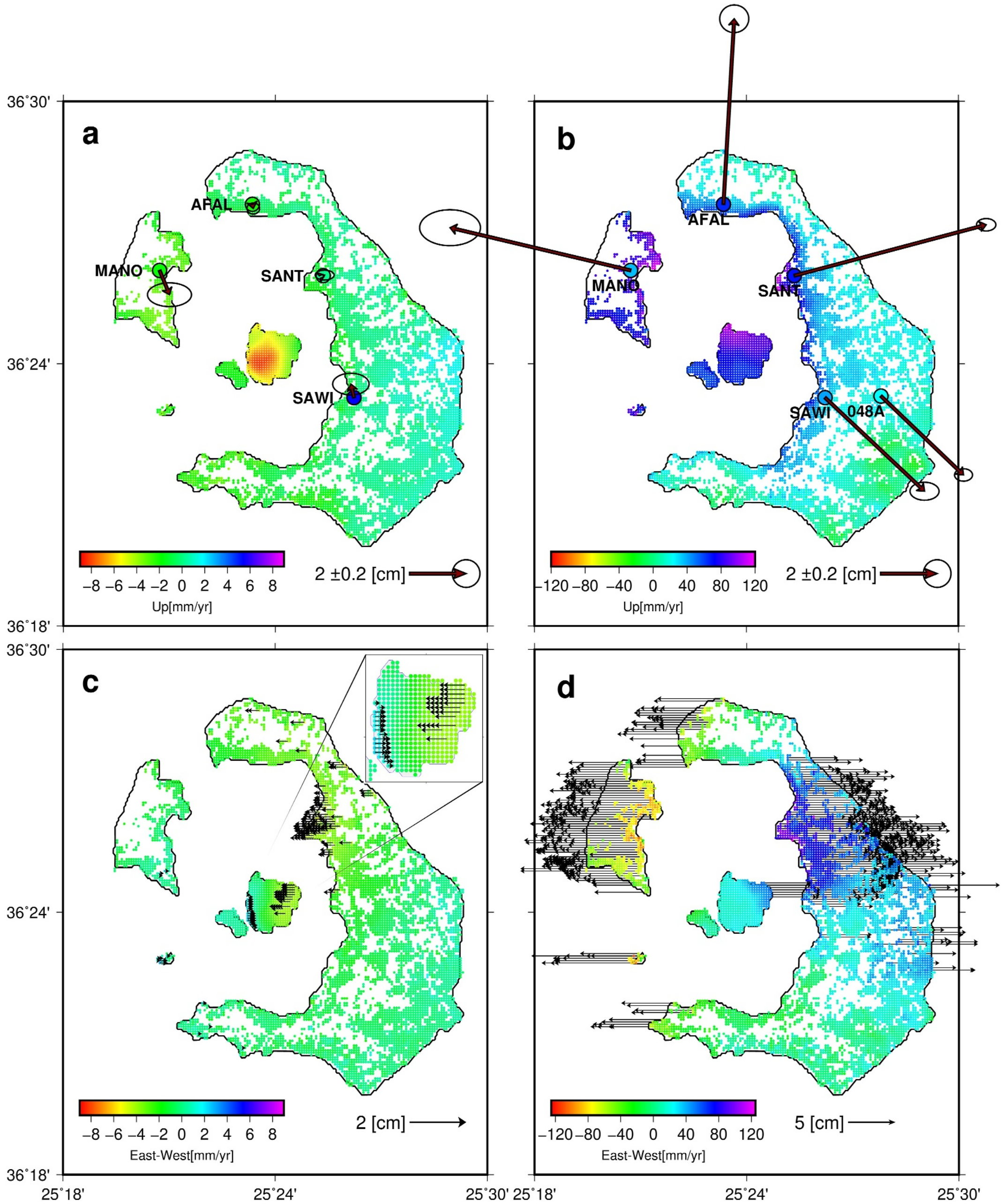

Figure 3. Sentinel-1 multi-temporal InSAR vertical (a, b) and E-W (c, d) motion rates before (04/2015–07/2024, a, and c) and during the unrest (07/2024–12/2024, b, and d). The E-W motion for points with higher rates is also depicted using vectors to highlight locations of major change. Vectors and colored circles at the GNSS station locations show horizontal and vertical velocities, respectively, before (01/2023–07/2024) (a) and during (07/2024–12/2024) (b) the 2024 unrest.

showing relatively narrow 1D distributions peaked on optimal values, without evident trade-offs in the 2D distributions.

Figure 4 presents a comparison between observed and model GNSS and InSAR data, as well the source position and its uncertainty. We observe a generally good model fit (Figures 4c and 4f), without extended trends of under- or over-estimation. Negative residuals can be observed in the northern part of Santorini for the descending orbit, while positive residuals areas are localized in Thirasia. The model also reproduces (within GNSS uncertainties) the horizontal and vertical deformation at SANT. Small deviations, compared to GNSS errors, are seen in the modeled deformation at SAWI and AFAL, while sites 048A and MANO show larger discrepancies.

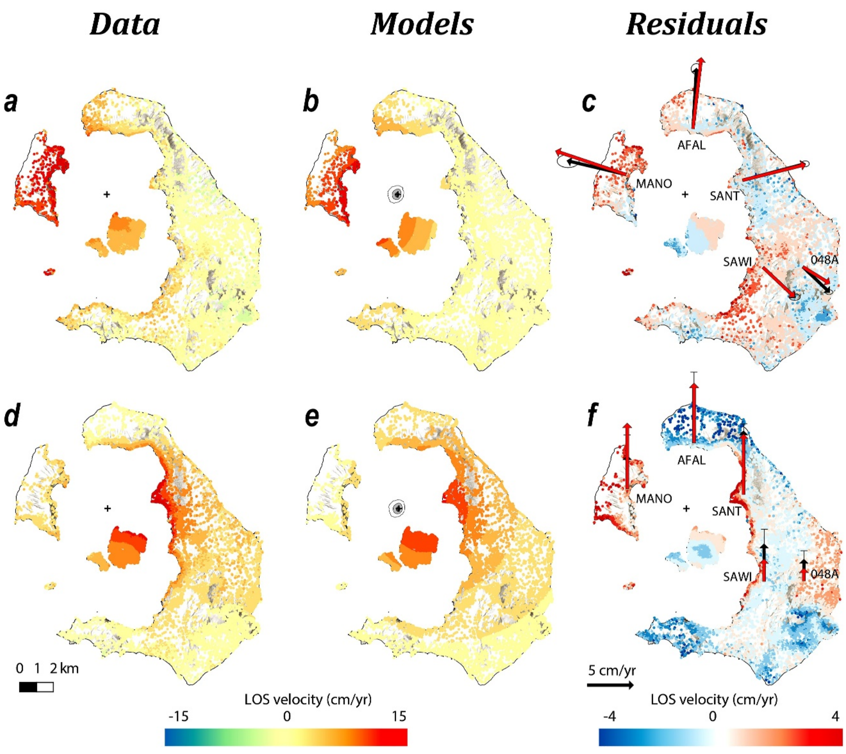

Figure 4. Ascending (a) and descending (d) mean synthetic aperture radar interferometry (InSAR) velocities and their comparison with the corresponding model velocities (b and e, respectively). (c) and (f) present the corresponding InSAR velocity residuals (observed minus modeled data), as well as the horizontal and vertical GNSS velocities, respectively (black vectors: observed data with horizontal error ellipses (c) and vertical errorbars (f), red vectors: modeled velocities). The inferred deformation source location is depicted with a cross, while model panels (b, f) present the 15%, 50%, and 85% confidence contours for its position.

5. Conclusions

Figure 5 presents a summary comparison of the 2011–2012 and the current intra-caldera unrests. Both occurrences involve a similar radial expansion from a deformation source within the northern Santorini caldera melt storage (dashed line in Figure 5), identified by tomography at the depth of 3–5 km as a low-velocity/low-density region, which facilitates magma ascent (e.g., Hooft et al., 2019). The magma source location and depth for the ongoing unrest is compatible with that of the 2011–2012 unrest within the model uncertainties (Foumelis et al., 2013; Newman et al., 2012; Parks et al., 2015; Saltogianni et al., 2014). Both sources also lie roughly along the Koloumbo line (Figure 1), a major tectonic feature with intense faulting and dike intrusion (e.g., Drymoni et al., 2020). The low-velocity anomaly (Figure 5) also extends toward the Kolumbo line (McVey et al., 2020) at shallower depths (2–4 km), which are compatible with the proposed depth range of the deformation source.

The observed deformation from GNSS and InSAR data (Figure 5), as well as the proposed volume variation rate of the current unrest (12.5×10^6 m^3/yr) are in the range of the 2011–2012 unrest, for which estimates vary between 6.4×10^6 m^3/yr (Foumelis et al., 2013) and $14–15 \times 10^6$ m^3/yr (Newman et al., 2012; Parks et al., 2012, 2015) for different source geometries. This rate is only an order of magnitude larger than the long-term magma inflow rate (~10^6 m^3/yr, Druitt et al., 2012), which also applies to the historical eruption period (e.g., Johnston et al., 2015; Nomikou et al., 2014), suggesting that the current unrest involves most of the magma accumulated during the 14-year inter-unrest period. Seismicity also shows activation of the same, near-vertical Kameni line fault, which remains almost completely silent between unrests. This fault has been activated further inland during the current unrest, with average fault plane solutions (using the approach of C.B. Papazachos and Kiratzi, 1992) indicating a NW-SE extension for both unrests. This pattern agrees with previous results (Dimitriadis et al., 2009; Papadimitriou et al., 2015), confirming the strong stress interaction between active faulting and volcanism, also suggested for the 2011–2012 unrest (e.g., Feuillet, 2013). However, the low seismicity level and the lack of

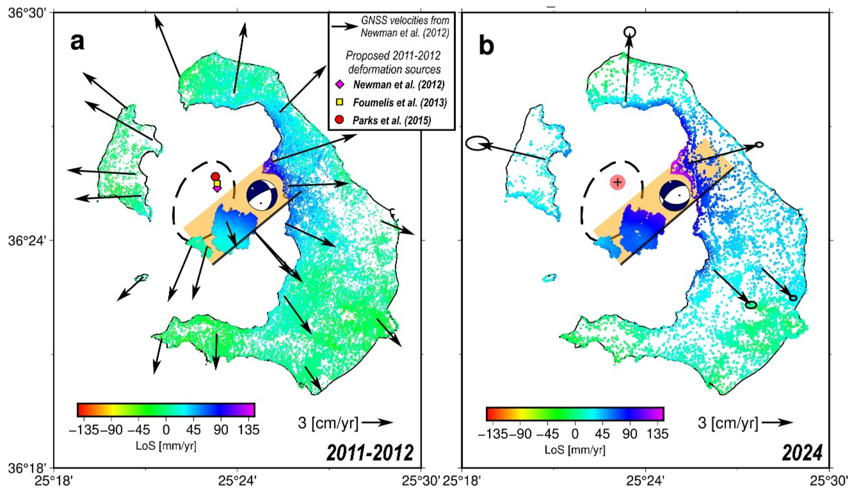

Figure 5. (a) GNSS velocities from Newman et al. (2012) and surface motion rates from MT-SAR analysis for the 2011–2012 unrest (03/2011–03/2012, Foumelis et al., 2013). b) Same information for the first phase of the 2024 unrest (07/2024–12/2024, this work). MT-SAR results are shown for descending tracks of ENVISAT for (a) and Sentinel-1 for (b). Colored symbols in (a) and the red area in (b) depict the proposed magma sources, located within the northern-caldere low-velocity anomaly (dashed line). The activated Kameni line fault segments (rectangle with upper fault edge shown with a solid line) and the corresponding average fault plane solutions are also presented.

differential InSAR displacements along the fault suggest that its activation did not affect the observed deformation pattern, similar to the 2011–2012 unrest and contrary to other volcanic areas (e.g., Vilardo et al., 2010).

Considering the long-term subsidence of Nea Kameni documented for 04/2015–07/2024, as well as before and after the previous unrest (Foumelis et al., 2013; Papageorgiou et al., 2019; Parks et al., 2013; Saltogianni et al., 2014), it is evident that Santorini experiences unrest episodes with sudden inflation onset and coeval (or slightly delayed) seismic swarms, accompanied by longer intervals of slow deflation between the unrest (Hooper, 2012). It is hard to assess if and when the current unrest will end (as in mid-2012) or if it will lead to an eruption. Inflation events for calderas like Santorini often last several years or more, sometimes with variable rates (e.g., Yamasaki et al., 2022). However, felsic calderas erupt rather infrequently, exhibiting short and seismically active unrests with uplift, suggesting repeated stalled intrusions (see Acocella et al., 2015 for a detailed review). Thermomechanical modeling for the magma chamber beneath Nea Kameni suggests that it contains little to no exsolved volatiles, requiring less than 1% of mass increase to reach the critical overpressure, hence resulting in small-scale eruptions (Degruyter et al., 2016), like those observed historically. However, since these eruptions had a small but important impact (e.g., Drymoni et al., 2023; Vougioukalakis & Fytikas, 2005), and as the steady rates of Figure 2 can be followed by increased deformation and magma intrusion, possibly leading to an eruption (e.g., Chadwick et al., 2012), improved spatial and temporal real-time monitoring of the volcano is required to identify any pre-eruptive patterns.

Conflict of Interest

The authors declare no conflicts of interest relevant to this study.

Data Availability Statement

Aristotle University seismological network (https://doi.org/10.7914/SN/HT, Aristotle University of Thessaloniki, 1981) earthquake data are available through its repository (https://seismo.auth.gr/general-earthquake-catalogs/), while original seismic waveforms of the HUSN are available through the Greek EIDA node, hosted at the National Observatory of Athens (https://eida.gein.noa.gr/fdsnws/dataselect/1/builder, European Integrated Data Archive, 2016). GNSS time series (Figure 2) are available at Zenodo and can be obtained via Papazachos et al. (2025): https://doi.org/10.5281/zenodo.15598671. H_2 data can be obtained from Zenodo via Tassi et al. (2025): https://doi.org/10.5281/zenodo.15602709 and have been collected with the procedure described by Tassi et al. (2013). Sentinel-1 Single Look Complex (SLC) acquisitions are from the Copernicus programme, accessible through the geobrowsers of the Copernicus Data Space Ecosystem (https://browser.dataspace.copernicus.eu/?zoom=5&lat=50.16282&lng=20.78613&themeId=DEFAULT-THEME&visualizationUrl=U2FsdGVkX18If5%2FLmGAx1j1nTH5pw%2Fhhdqqrx8hGEBrkDY6Q%2FIVW9jYFESKPAg34ggsJ9BRfM6Cy1SXSWpTcQRT649IO0WqgDcSguGfRKnWBTDMAk03ajIRBEPFRnEwZ&datasetId=S2_L2A_CDAS) and the Alaska Satellite Facility (https://search.asf.alaska.edu/#/, Copernicus Sentinel-1 data, 2015–2024); access to the data is provided after free registration. The SNAPPING service (Foumelis et al., 2022) is available on the Geohazards Exploitation Platform (GEP; https://geohazards-tep.eu) after free registration; access to the service is provided through custom links by the service operators after the registration. The open-source Volcanic and Seismic source Modelling (VSM) Python tool (Trasatti, 2022) is freely available on GitHub (https://github.com/EliTras/VSM) and is accompanied by step-by-step documentation in Jupyter Notebooks. The GAMIT-GLOBK (Version 10.71) software (Herring et al., 2015) is available from https://www-gpsg.mit.edu/gg/ and is provided without written agreement or royalty fee by universities and government agencies for non-commercial education and research purposes after a license request (https://geoweb.mit.edu/gg/license.php). Figures have been produced using the Generic Mapping Tools (GMT) software v6.0.0 (Wessel et al., 2019), as well as the open-source Inkscape software (https://inkscape.org/, Inkscape, 2025).

Acknowledgments

We thank the Hellenic Cadaster and Metrica SA for providing data/services of the HEPOS station 048A and HxGN/SmartNet-Greece station SANT, respectively. This work contains modified Copernicus Sentinel-1 mission data (2015–2024). ISMOSAV networks are partly supported by Geothira MAE and AUTh (Project11097-ELKE_AUTh and Project13178-ELKE_AUTh). We would like to thank GRL Editor Christian Huber and reviewers Paul Lundgren and Maurizio Battaglia for their valuable comments and suggestions.

References

Acocella, V., Di Lorenzo, R., Newhall, C., & Scandone, R. (2015). An overview of recent (1988 to 2014) caldera unrest: Knowledge and perspectives. *Reviews of Geophysics*, *53*(3), 896–955. https://doi.org/10.1002/2015rg000492

Altamimi, Z., Rebischung, P., Metivier, L., & Collilieux, X. (2016). ITRF2014: A new release of the international terrestrial reference frame modeling nonlinear station motions. *Journal of Geophysical Research: Solid Earth*, *121*(8), 6109–6131. https://doi.org/10.1002/2016JB013098

Aristotle University of Thessaloniki. (1981). Aristotle university of Thessaloniki seismological network [Dataset]. *International Federation of Digital Seismograph Networks*. https://doi.org/10.7914/SN/HT

Battaglia, M., Cervelli, P. F., & Murray, J. R. (2013). Modeling crustal deformation near active faults and volcanic centers—a catalog of deformation models. Retrieved from http://pubs.er.usgs.gov/publication/tm13B1

Bitharis, S., Pikridas, C., Fotiou, A., & Rossikopoulos, D. (2024). GPS data analysis and geodetic velocity field investigation in Greece, 2001–2016. *GPS Solutions*, *28*(1), 16. https://doi.org/10.1007/s10291-023-01549-8

Bruyninx, C., Legrand, J., Fabian, A., & Pottiaux, E. (2019). GNSS metadata and data validation in the EUREF permanent network. *GPS Solutions*, *23*(4), 106. https://doi.org/10.1007/s10291-019-0880-9

Chadwick, W. W., Jr., Nooner, S. L., Butterfield, D. A., & Lilley, M. D. (2012). Seafloor deformation and forecasts of the April 2011 eruption at axial seamount. *Nature Geoscience*, *5*(7), 474–477. https://doi.org/10.1038/ngeo1464

Copernicus Sentinel-1 data. (2015–2024). Data provided by the European union and the European space agency (ESA) under the Copernicus programme [Dataset]. *European Space Agency*. Retrieved from https://dataspace.copernicus.eu/

Degruyter, W., Huber, C., Bachmann, O., Cooper, K. M., & Kent, A. J. (2016). Magma reservoir response to transient recharge events: The case of Santorini volcano (Greece). *Geology*, *44*(1), 23–26. https://doi.org/10.1130/g37333.1

Dimitriadis, I., Karagianni, E., Panagiotopoulos, D. G., Papazachos, C. B., Hatzidimitriou, P., Bohnhoff, M., et al. (2009). Seismicity and active tectonics at Coloumbo reef (Aegean sea, Greece): Monitoring an active volcano at Santorini volcanic center using a temporary seismic network. *Tectonophysics*, *465*(1–4), 136–149. https://doi.org/10.1016/j.tecto.2008.11.005

Dimitriadis, I., Papazachos, C., Panagiotopoulos, D., Hatzidimitriou, P., Bohnhoff, M., Rische, M., & Meier, T. (2010). P and S velocity structures of the Santorini-Coloumbo volcanic system (Aegean Sea, Greece) obtained by non-linear inversion of travel times and its tectonic implications. *Journal of Volcanology and Geothermal Research*, *195*(1), 13–30. https://doi.org/10.1016/j.jvolgeores.2010.05.013

Dimitriadis, I. M., Panagiotopoulos, D. G., Papazachos, C. B., Hatzidimitriou, P. M., Karagianni, E. E., & Kane, I. (2005). Recent seismic activity (1994-2002) of the Santorini volcano using data from local seismological network. *Developments in Volcanology: The South Aegean Volcanic Arc*, *391*, 185–204.

Druit, T. H., Pyle, D. M., & Mather, T. A. (2019). Santorini Volcano and its plumbing system. *Elements*, *15*(3), 177–184. https://doi.org/10.2138/gselements.15.3.177

Druitt, T. H., Costa, F., Deloule, E., Dungan, M., & Scaillet, B. (2012). Decadal to monthly timescales of magma transfer and reservoir growth at a caldera volcano. *Nature*, *482*(7383), 77–80. https://doi.org/10.1038/nature10706

Drymoni, K., Browning, J., & Gudmundsson, A. (2020). Dyke-arrest scenarios in extensional regimes: Insights from field observations and numerical models, Santorini, Greece. *Journal of Volcanology and Geothermal Research*, *396*, 106854. https://doi.org/10.1016/j.jvolgeores.2020.106854

Drymoni, K., Browning, J., Pomonis, P., & Magganas, A. (2023). Historical accounts provide insight on the geological evolution of the 20th century eruptions at Santorini volcano, Greece. *Bulletin of Volcanology*, *85*(12), 70. https://doi.org/10.1007/s00445-023-01681-w

European Integrated Data Archive. (2016). European integrated data archive (EIDA) node at the Institute of geodynamics of the national observatory of Athens [Dataset]. *Institute of Geodynamics of the National Observatory of Athens*. Retrieved from https://eida.gein.noa.gr/

Feuillet, N. (2013). The 2011–2012 unrest at Santorini rift: Stress interaction between active faulting and volcanism. *Geophysical Research Letters*, *40*(14), 3532–3537. https://doi.org/10.1002/grl.50516

Foumelis, M. (2016). Vector-based approach for combining ascending and descending persistent scatterers interferometric point measurements. *Geocarto International*, *33*(1), 38–52. https://doi.org/10.1080/10106049.2016.1222636

Foumelis, M., Delgado Blasco, J. M., Brito, F., Pacini, F., Papageorgiou, E., Pishehvar, P., & Bally, P. (2022). SNAPPING services on the Geohazards exploitation platform for Copernicus Sentinel-1 surface motion mapping. *Remote Sensing*, *14*(23), 6075. https://doi.org/10.3390/rs14236075

Foumelis, M., Trasatti, E., Papageorgiou, E., Stramondo, S., & Parcharidis, I. (2013). Monitoring Santorini volcano (Greece) breathing from space. *Geophysical Journal International*, *193*(1), 161–170. https://doi.org/10.1093/gji/ggs135

Georgalas, G. (1953). L' éruption du volcan de Santorini en 1950. *Bulletin of Volcanology*, *13*(1), 39–55. https://doi.org/10.1007/bf02596790

Heath, B. A., Hooft, E. E. E., Toomey, D. R., Papazachos, C. B., Nomikou, P., Paulatto, M., et al. (2019). Tectonism and its relation to magmatism around Santorini Volcano from upper crustal P wave velocity. *Journal of Geophysical Research: Solid Earth*, *124*(10), 10610–10629. https://doi.org/10.1029/2019jb017699

Herring, T. A., King, R. W., Floyd, M. A., & McClusky, S. C. (2015). GAMIT reference manual [Software]. *GPS Analysis at MIT*. https://www-gpsg.mit.edu/gg/

Hooft, E. E. E., Heath, B. A., Toomey, D. R., Paulatto, M., Papazachos, C. B., Nomikou, P., et al. (2019). Seismic imaging of Santorini: Subsurface constraints on caldera collapse and present-day magma recharge. *Earth and Planetary Science Letters*, *514*, 48–61. https://doi.org/10.1016/j.epsl.2019.02.033

Hooper, A. (2012). A volcano's sharp intake of breath. *Nature Geoscience*, *5*(10), 686–687. https://doi.org/10.1038/ngeo1584

Inkscape. (2025). The Inkscape project (version 1.4.2) [Software]. *Inkscape*. Retrieved from https://inkscape.org/

Johnston, E. N., Sparks, R. S. J., Nomikou, P., Livanos, I., Carey, S., Phillips, J. C., & Sigurdsson, H. (2015). Stratigraphic relations of Santorini's intracaldera fill and implications for the rate of post-caldera volcanism. *Journal of the Geological Society*, *172*(3), 323–335. https://doi.org/10.1144/jgs2013-114

Klein, F. W. (2002). *User's guide to HYPOINVERSE-2000, a Fortran program to solve for earthquake locations and magnitudes* (pp.171). US Geological Survey, Publ.

McVey, B. G., Hooft, E. E. E., Heath, B. A., Toomey, D. R., Paulatto, M., Morgan, J. V., et al. (2020). Magma accumulation beneath Santorini volcano, Greece, from P-wave tomography. *Geology*, *48*(3), 231–235. https://doi.org/10.1130/g47127.1

Newman, A. V., Stiros, S., Feng, L., Psimoulis, P., Moschas, F., Saltogianni, V., et al. (2012). Recent geodetic unrest at Santorini caldera, Greece. *Geophysical Research Letters*, *39*(6), L06309. https://doi.org/10.1029/2012gl051286

Nomikou, P., Parks, M. M., Papanikolaou, D., Pyle, D. M., Mather, T. A., Carey, S., et al. (2014). The emergence and growth of a submarine volcano: The Kameni islands, Santorini (Greece). *Geographical Research J.*, *1*, 8–18. https://doi.org/10.1016/j.grj.2014.02.002

Papadimitriou, P., Kapetanidis, V., Karakonstantis, A., Kaviris, G., Voulgaris, N., & Makropoulos, K. (2015). The Santorini volcanic complex: A detailed multi-parameter seismological approach with emphasis on the 2011–2012 unrest period. *Journal of Geodynamics*, *85*, 32–57. https://doi.org/10.1016/j.jog.2014.12.004

Papageorgiou, E., Foumelis, M., & Parcharidis, I. (2012). Long-and short-term deformation monitoring of Santorini Volcano: Unrest evidence by DInSAR analysis. *IEEE Journal of Selected Topics in Applied Earth Observations and Remote Sensing*, *5*(5), 1531–1537. https://doi.org/10.1109/jstars.2012.2198871

Papageorgiou, E., Foumelis, M., Trasatti, E., Ventura, G., Raucoules, D., & Mouratidis, A. (2019). Multi-sensor SAR geodetic imaging and modelling of Santorini Volcano post-unrest response. *Remote Sensing*, *11*(3), 259. https://doi.org/10.3390/rs11030259

Papazachos, C., Foumelis, M., Bitharis, S., Pikridas, C., Trasatti, E., Papageorgiou, E., et al. (2025). GNSS time series for the initial phase of the 2024-2025 intra-caldera unrest in Santorini [Dataset]. *Zenodo*. https://doi.org/10.5281/zenodo.15598671

Papazachos, C. B., & Kiratzi, A. A. (1992). A formulation for reliable estimation of active crustal deformation and its application to central Greece. *Geophysical Journal International*, *111*(3), 424–432. https://doi.org/10.1111/j.1365-246X.1992.tb02101.x

Papazachos, C. B., & Nolet, G. (1997). P and S deep velocity structure of the Hellenic area obtained by robust non-linear inversion of travel times. *Journal of Geophysical Research*, *102*(B4), 8349–8367. https://doi.org/10.1029/96JB03730

Parks, M. M., Biggs, J., England, P., Mather, T. A., Nomikou, P., Palamartchouk, K., et al. (2012). Evolution of Santorini Volcano dominated by episodic and rapid fluxes of melt from depth. *Nature Geoscience*, *5*(10), 749–754. https://doi.org/10.1038/ngeo1562

Parks, M. M., Caliro, S., Chiodini, G., Pyle, D. M., Mather, T. A., Berlo, K., et al. (2013). Distinguishing contributions to diffuse CO2 emissions in volcanic areas from magmatic degassing and thermal decarbonation using soil gas 222Rn-δ13C systematics: Application to Santorini volcano, Greece. *Earth and Planetary Science Letters*, *377–378*, 180–190. https://doi.org/10.1016/j.epsl.2013.06.046

Parks, M. M., Moore, J. D., Papanikolaou, X., Biggs, J., Mather, T. A., Pyle, D. M., et al. (2015). From quiescence to unrest: 20 years of satellite geodetic measurements at Santorini volcano, Greece. *Journal of Geophysical Research: Solid Earth*, *120*(2), 1309–1328. https://doi.org/10.1002/2014jb011540

Pearson, C. L., Brewer, P. W., Brown, D., Heaton, T. J., Hodgins, G. W., Jull, A. T., et al. (2018). Annual radiocarbon record indicates 16th century BCE date for the Thera eruption. *Science Advances*, *4*(8), eaar8241. https://doi.org/10.1126/sciadv.aar8241

Pyle, D. M., & Elliott, J. R. (2006). Quantitative morphology, recent evolution, and future activity of the Kameni Islands volcano, Santorini, Greece. *Geosphere*, *2*(5), 253–268. https://doi.org/10.1130/ges00028.1

Saltogianni, V., Stiros, S. C., Newman, A. V., Flanagan, K., & Moschas, F. (2014). Time-space modeling of the dynamics of Santorini volcano (Greece) during the 2011-2012 unrest. *Journal of Geophysical Research: Solid Earth*, *119*(11), 8517–8537. https://doi.org/10.1002/2014JB011409

Scordilis, E. M., Kementzetzidou, D., & Papazachos, B. C. (2016). Local magnitude calibration of the Hellenic unified seismic network. *Journal of Seismology*, *20*(1), 319–332. https://doi.org/10.1007/s10950-015-9529-5

Stiros, S. C., Psimoulis, P., Vougioukalakis, G., & Fyticas, M. (2010). Geodetic evidence and modeling of slow, small-scale inflation episode in the Thera (Santorini) volcano caldera, Aegean Sea. *Tectonophysics*, *494*(3–4), 180–190. https://doi.org/10.1016/j.tecto.2010.09.015

Tassi, F., Nisi, B., & Vaselli, O. (2025). H2 emissions at Nea Kameni fumaroles (NK1, NK3, NK5) and hot springs (AN) for the period 2010-2024 [Dataset]. *Zenodo*. https://doi.org/10.5281/zenodo.15602709

Tassi, F., Vaselli, O., Papazachos, C. B., Giannini, L., Chiodini, G., Vougioukalakis, G. E., et al. (2013). Geochemical and isotopic changes in the fumarolic and submerged gas discharges during the 2011-2012 unrest at Santorini caldera (Greece). *Bulletin of Volcanology*, *75*(4), 711. https://doi.org/10.1007/s00445-013-0711-8

Trasatti, E. (2022). Volcanic and seismic source modeling: An open tool for geodetic data modeling. *Frontiers in Earth Science*, *10*. https://doi.org/10.3389/feart.2022.917222

Vilardo, G., Isaia, R., Ventura, G., De Martino, P., & Terranova, C. (2010). InSAR Permanent Scatterer analysis reveals fault re-activation during inflation and deflation episodes at Campi Flegrei caldera. *Remote Sensing of Environment*, *114*(10), 2373–2383. https://doi.org/10.1016/j.rse.2010.05.014

Vougioukalakis, G., & Fytikas, M. (2005). Volcanic hazards in the Aegean area, relative risk evaluation, monitoring and present state of the active volcanic centers. In M. Fytikas & G. Vougioukalakis (Eds.), *The South Aegean active Volcanic Arc – present knowledge and future perspectives* (Vol. 7, pp. 161–183). Elsevier Series Developments in Volcanology. https://doi.org/10.1016/s1871-644x(05)80037-3

Vougioukalakis, G., Sparks, R. S., Druitt, T., Pyle, D., Papazachos, C., & Fytikas, M. (2016). Volcanic hazard assessment at Santorini Volcano: A review and a synthesis in the light of the 2011-2012 Santorini unrest. *Bulletin of the Geological Society of Greece*, *50*(1), 274–283. https://doi.org/10.12681/bgsg.11728

Waldhauser, F., & Ellsworth, W. L. (2000). A double-difference earthquake location algorithm: Method and application to the northern Hayward fault, California. *Bulletin of the Seismological Society of America*, *90*(6), 1353–1368.
Wegmüller, U., Werner, C., Strozzi, T., Wiesmann, A., Frey, O., & Santoro, M. (2015). Sentinel-1 IWS mode support in the GAMMA software, In *Proceedings of the 2015 IEEE 5th Asia-Pacific conference on synthetic aperture radar, APSAR 2015* (pp. 431–436). Institute of Electrical and Electronics Engineers Inc.
Werner, C., Wegmüller, U., Strozzi, T., & Wiesmann, A. (2003). Interferometric point target analysis for deformation mapping, In *IEEE International Geoscience Remote Sensing Symposium* (Vol. 7, pp. 4362–4364).
Wessel, P., Luis, J. F., Uieda, L., Scharroo, R., Wobbe, F., Smith, W. H. F., & Tian, D. (2019). The generic mapping tools version 6 [Software]. *Geochemistry, Geophysics, Geosystems*, *20*(11), 5556–5564. https://doi.org/10.1029/2019GC008515
Yamasaki, T., Sigmundsson, F., & Iguchi, M. (2022). Variable inflation rate of a magmatic deformation source beneath Aira caldera after the 1914 eruption of Sakurajima volcano: Inferences from a linear Maxwell viscoelastic model constrained by geodetic data. *Journal of Volcanology and Geothermal Research*, *421*, 107446. https://doi.org/10.1016/j.jvolgeores.2021.107446
Yang, X. M., Davis, P. M., & Dieterich, J. H. (1988). Deformation from inflation of a dipping finite prolate spheroid in an elastic half-space as a model for volcanic stressing. *Journal of Geophysical Research*, *93*(B5), 4249–4257. https://doi.org/10.1029/jb093ib05p04249